PLANE WAVE DIFFRACTION BY A STRIP WITH DIFFERENT SURFACE IMPEDANCES: PART I — THE CASE OF E POLARIZATON

Teruhisa Tsushima[1], Kazuya Kobayashi[1]*, Eldar I. Veliev[2], and Shoichi Koshikawa[3]

[1] Department of Electrical and Electronic Engineering, Chuo University
1-13-27 Kasuga, Bunkyo-ku, Tokyo 112-8551, Japan
[2] Institute of Radiophysics and Electronics, National Academy of Sciences
Ulitsa Proskury 12, Kharkov 310085, Ukraine
[3] Antenna Giken Co., Ltd., 4-72 Miyagayato, Omiya 330-0011, Japan

1. Introduction

Analysis of the diffraction by imperfectly conducting and absorbing strips is important in electromagnetic theory, and it is relevant to many engineering applications such as antenna and radar cross section (RCS) studies. This structure serves as a suitable model of finite metal-backed dielectric layers and dielectric-coated wires. The diffraction by strips with impedance and related approximate boundary conditions has been investigated thus far using function-theoretic and high-frequency methods [1–3]. In [4], we have analyzed the plane wave diffraction by a two-dimensional (2-D) resistive strip using the analytical-numerical approach based on the orthogonal polynomial expansion in conjunction with the Fourier transform [5], where the efficient solution has been obtained for the same resistivity on both sides of the strip. It is to be noted that our analytical-numerical approach is entirely different from the methods employed previously for analyzing scattering problems related to the impedance strip. In this two-part paper, we shall consider a 2-D strip with different impedances on its two surfaces as an important generalization to our previous analysis, and solve the plane wave diffraction rigorously using the analytical-numerical approach. The first part concerns the case of E polarization.

Applying the boundary condition to an integral representation of the scattered field, the problem is formulated as simultaneous integral equations satisfied by the electric and magnetic current density functions. We shall then take the Fourier transform of the integral equations and expand the unknown current density functions into the infinite series containing the Chebyshev polynomials. This leads to two infinite systems of linear algebraic equations (SLAE) satisfied by the expansion coefficients. These coefficients are determined numerically with high accuracy via appropriate truncation of the SLAE. Evaluating the scattered field asymptotically, a far field expression is derived. We shall present illustrative numerical examples on the monostatic and bistatic RCS, and discuss the far field scattering characteristics. Some comparisons with Tiberio *et al.* [3] are also given to validate the present method.

The time factor is assumed to be $e^{-i\omega t}$ and suppressed throughout the following analysis.

2. Formulation of the Problem

We consider the E-polarized plane wave diffraction by a 2-D impedance strip of zero thickness as shown in Fig. 1, where ζ_1 and ζ_2 denote the normalized impedance of the upper and lower surfaces of the strip, respectively. Let the total electric field $E_z(x,y)$ be

$$E_z(x,y) = E_z^i(x,y) + E_z^s(x,y), \tag{1}$$

where $E_z^i(x,y)$ is the incident field given by

$$E_z^i(x,y) = e^{-ik(x\alpha_0 + y\sqrt{1-\alpha_0^2})}, \quad \alpha_0 = \cos\theta \tag{2}$$

for $0 \le \theta \le \pi$ with k [$\equiv \omega(\mu_0\varepsilon_0)^{1/2}$] being the free-space wavenumber. The total field satisfies the boundary condition as given by

$$\frac{\partial E_z(x,\pm 0)}{\partial y} \pm \frac{ik}{\zeta_{1,2}} E_z(x,\pm 0) = 0, \quad |x| < a. \tag{3}$$

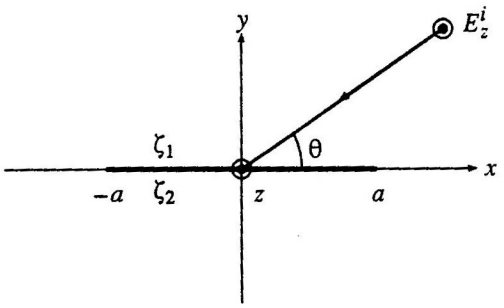

Fig. 1. Geometry of the problem.

Using Green's formula, we can express the scattered field $E_z^s(x,y)$ in (1) as

$$E_z^s(x,y) = -\frac{i}{4}\int_{-a}^{a}\left\{f_1(x') + f_2(x')\frac{\partial}{\partial y}\right\}H_0^{(1)}\left(k\sqrt{(x-x')^2+y^2}\right)dx' \tag{4}$$

with $H_0^{(1)}(\cdot)$ being the Hankel function of the first kind, where $f_1(x)$ and $f_2(x)$ are the unknown electric and magnetic current density functions, respectively, which are defined by

$$f_1(x) = \frac{\partial E_z(x,+0)}{\partial y} - \frac{\partial E_z(x,-0)}{\partial y}, \quad f_2(x) = E_z(x,+0) - E_z(x,-0). \tag{5}$$

Taking into account the boundary condition as given by (3), we obtain from (1), (2), and (4) that

$$\frac{Z_1}{k}f_1(x) + Z_2 f_2(x) = 2ie^{-ikx\alpha_0} + \frac{1}{2}\int_{-a}^{a} f_1(x')H_0^{(1)}\left(k|x-x'|\right)dx', \tag{6a}$$

$$-Z_2 f_1(x) + kZ_3 f_2(x) = 2k\sqrt{1-\alpha_0^2}e^{-ikx\alpha_0} + \frac{1}{2}\lim_{y\to 0}\frac{\partial^2}{\partial y^2}\int_{-a}^{a} f_2(x')H_0^{(1)}\left(k\sqrt{(x-x')^2+y^2}\right)dx', \tag{6b}$$

where

$$Z_1 = -\frac{2\zeta_1\zeta_2}{\zeta_1+\zeta_2}, \quad Z_2 = \frac{i(\zeta_1-\zeta_2)}{\zeta_1+\zeta_2}, \quad Z_3 = \frac{2}{\zeta_1+\zeta_2}. \tag{7}$$

Equations (6a,b) are the integral equations to this diffraction problem.

3. Solution of the Integral Equations

We multiply both sides of (6a,b) by $e^{-ikz\beta}$ and integrate with respect to x for $-a < x < a$. Carrying out some manipulations with the aid of the Fourier integral representation of the Hankel function, it follows that

$$\frac{Z_1F_1(\beta)}{\kappa} + Z_2F_2(\beta) = 4i\frac{\sin\kappa(\alpha_0+\beta)}{\kappa(\alpha_0+\beta)} + \frac{1}{\pi}\int_{-\infty}^{\infty}F_1(\alpha)\frac{\sin\kappa(\alpha-\beta)}{\kappa(\alpha-\beta)}\frac{d\alpha}{\sqrt{1-\alpha^2}}, \tag{8a}$$

$$-\frac{Z_2F_1(\beta)}{\kappa} + Z_3F_2(\beta) = 4\sqrt{1-\alpha_0^2}\frac{\sin\kappa(\alpha_0+\beta)}{\kappa(\alpha_0+\beta)} - \frac{1}{\pi}\int_{-\infty}^{\infty}F_2(\alpha)\frac{\sin\kappa(\alpha-\beta)}{\alpha-\beta}\sqrt{1-\alpha^2}d\alpha, \tag{8b}$$

where

$$F_1(\alpha) = a\int_{-1}^{1}f_1(a\eta)e^{-i\kappa\alpha\eta}d\eta, \quad F_2(\alpha) = \int_{-1}^{1}f_2(a\eta)e^{-i\kappa\alpha\eta}d\eta \tag{9}$$

with $\kappa = ka$ and $x = a\eta$. It can be shown that $f_{1,2}(x)$ in (5) are expanded in the form

$$f_1(x) = \frac{1}{a\sqrt{1-(x/a)^2}}\left\{f_0^1 + 2\sum_{n=1}^{\infty}\frac{f_n^1}{n}T_n\left(\frac{x}{a}\right)\right\}, \quad f_2(x) = \sqrt{1-\left(\frac{x}{a}\right)^2}\sum_{n=0}^{\infty}f_n^2U_n\left(\frac{x}{a}\right), \tag{10}$$

where $T_n(\cdot)$ and $U_n(\cdot)$ denote the Chebyshev polynomial of the first and second kinds, respectively. In (10), $f_n^{1,2}$ for $n = 0, 1, 2, \cdots$ are unknown coefficients to be determined. Substituting (10) into (8a,b) and applying some properties of the Weber–Schafheitlin discontinuous integrals, we derive the two infinite systems of linear algebraic equations (SLAE) as in

$$\sum_{n=0}^{\infty}x_n^1(Z_1d_{mn}^0 - c_{mn}) + Z_2\sum_{n=0}^{\infty}x_n^2d_{mn}^1 = 4i\gamma_m, \tag{11a}$$

$$-Z_2\sum_{n=0}^{\infty}x_n^1d_{mn}^0 + \sum_{n=0}^{\infty}x_n^2(Z_3d_{mn}^1 + b_{mn}) = 4\sqrt{1-\alpha_0^2}\gamma_m \tag{11b}$$

for $m = 0, 1, 2, \cdots$, where

$$x_0^1 = f_0^1, \; x_n^1 = 2(-i)^nf_n^1/n \;\text{ for } n = 1, 2, 3, \cdots; \; x_n^2 = (-i)^n(n+1)f_n^2 \;\text{ for } n = 0, 1, 2, \cdots, \tag{12}$$

$$\gamma_m = (-1)^m\frac{J_{m+1}(\kappa\alpha_0)}{\alpha_0}, \tag{13}$$

$$b_{mn} = \{1+(-1)^{2K}\}\frac{\kappa^2}{4}\left(\kappa^{2K}\sum_{p=0}^{\infty}\frac{\delta_{p1}^1}{\Gamma(p+K+2)}\kappa^{2p} + \frac{i}{\pi}\left[-\sum_{p=0}^{K-1}\frac{\delta_{p1}^2}{\Gamma(p+2)}\kappa^{2p}\right.\right.$$
$$\left.\left.+\kappa^{2K}\sum_{p=0}^{\infty}\frac{\{C_{p1}-\Psi(p+K+2)\}\delta_{p1}^1}{\Gamma(p+K+2)}\kappa^{2p}\right]\right), \quad (m+n\text{: even}), \tag{14a}$$

$$c_{mn} = \{1+(-1)^{2K}\}\frac{\kappa}{2}\left(\kappa^{2K}\sum_{p=0}^{\infty}\frac{\delta_{p0}^1}{\Gamma(p+K+1)}\kappa^{2p} + \frac{i}{\pi}\left[-u_K\sum_{p=0}^{K-1}\frac{\delta_{p0}^2}{\Gamma(p+1)}\kappa^{2p}\right.\right.$$
$$\left.\left.+\kappa^{2K}\sum_{p=0}^{\infty}\frac{\{C_{p0}-\Psi(p+K+1)\}\delta_{p0}^1}{\Gamma(p+K+1)}\kappa^{2p}\right]\right), \quad (m+n\text{: even}), \tag{14b}$$

$$d^0_{mn} = \{1+(-1)^{2K}\}\frac{\Gamma(K+1/2)}{2\Gamma(K-m+1/2)\Gamma(K+3/2)\Gamma(K-n+3/2)}, \tag{15a}$$

$$d^1_{mn} = \{1+(-1)^{2K}\}\frac{\kappa\Gamma(K+1/2)}{4\Gamma(K-m+3/2)\Gamma(K+5/2)\Gamma(K-n+3/2)}, \tag{15b}$$

$$\delta^1_{p\lambda} = (-1)^p\frac{\Gamma(p+K+1/2)\Gamma(p+K+\lambda/2+1)\Gamma(p+K+\lambda/2+3/2)}{\Gamma(p+1)\Gamma(p+n+\lambda+1)\Gamma(p+m+2)\Gamma(p+2K+\lambda+2)}, \tag{16a}$$

$$\delta^2_{p\lambda} = \frac{\Gamma(-p+K)\Gamma(p+1/2)\Gamma(p+\lambda/2+1)\Gamma(p+\lambda/2+3/2)}{\Gamma(p-K+n+\lambda+1)\Gamma(p-K+m+2)\Gamma(p+K+\lambda+2)}, \tag{16b}$$

$$\begin{aligned} C_{p\lambda} = {} & 2\ln\kappa + \Psi(p+K+1/2) + \Psi(p+K+\lambda/2+1) + \Psi(p+K+\lambda/2+3/2) \\ & -\Psi(p+1) - \Psi(p+n+\lambda+1) - \Psi(p+m+2) - \Psi(p+2K+\lambda+2), \end{aligned} \tag{17}$$

$$u_0 = 0, \quad u_K = 1 \text{ for } K \geq 1 \text{ with } K = (m+n)/2. \tag{18}$$

In the above, $\Gamma(\cdot)$ and $J_{m+1}(\cdot)$ denote the gamma function and the Bessel function, respectively, and $\Psi(\cdot)$ is the logarithmic derivative of the gamma function. The unknowns $x^{1,2}_n$ can be determined with high accuracy by solving (11a,b) numerically via a truncation procedure.

4. Scattered Far Field

Substituting the asymptotic representation of the Hankel function into (4) and carrying out some manipulations with the aid of (10), we derive the scattered far field with the result that

$$E^s_z(r,\phi) \sim \sqrt{\frac{2}{\pi kr}}e^{i(kr-\pi/4)}\Phi(\phi), \quad kr \to \infty, \tag{19}$$

where (r,ϕ) is the cylindrical coordinate defined by $x = r\cos\phi$, $y = r\sin\phi$ for $-\pi \leq \phi \leq \pi$, and

$$\Phi(\phi) = -\frac{i\pi}{4}\sum_{n=0}^{\infty} x^1_n J_n(\kappa\cos\phi) + \frac{\pi}{4}\tan\phi\sum_{n=0}^{\infty} x^2_n J_{n+1}(\kappa\cos\phi). \tag{20}$$

5. Numerical Results and Discussion

We shall now investigate the far field scattering characteristics of the strip via numerical computation of the RCS. Figure 2 illustrates the monostatic RCS as a function of incidence angle θ for $ka = 5.0, 15.0$. In order to investigate the effect of the surface impedance on the scattered far field, four different cases have been considered as in $(\zeta_1,\zeta_2) = (0.0,0.0), (1.5,3.0), (1.5,1.5), (3.0,3.0)$, where $\zeta_{1,2} = 0.0$ corresponds to a perfectly conducting strip. Comparing the results for the impedance strip with those for the perfectly conducting strip, the RCS is reduced for the case of the impedance strip as expected. From the three RCS curves for the impedance strip, it is seen that the backscattered far field is not much affected by the impedance of the strip surface in the shadow region except near $\theta = 0°$. Shown in Fig. 3 is the bistatic RCS as a function of observation angle ϕ for $\theta = 60°$ and $ka = 5.0, 15.0$. It is seen that the RCS level of the impedance strip is lower than the perfectly conducting case for $-180° < \phi < -150°$ and $-60° < \phi < 180°$, whereas all the four curves are close to each other for $-150° < \phi < -60°$. It is therefore inferred that the scattered far field in the neighborhood of the incident shadow boundary ($\phi = -120°$) does not depend on the surface impedance of the strip. Figure 4 shows comparison with the results obtained by Tiberio *et al.* [3] using the geometrical theory of diffraction (GTD) together with the Maliuzhinetz method, where the bistatic RCS is illustrated as a function of observation angle ϕ for $\theta = 180°$, $ka = 10.0$, and $(\zeta_1,\zeta_2) = (4.0,0.0)$. It is seen from the figure that our RCS results are in excellent agreement with the results presented in [3].

Acknowledgments

The authors would like to thank Mr. Masanori Ogata, a former graduate school student at Chuo University, for assisting in the preparation of the manuscript. This work was supported in part by the 1997 Chuo University Special Research Grant and by the Institute of Science and Engineering, Chuo University.

References

[1] T. B. A. Senior, "Backscattering by a resistive strip," *IEEE Trans. Antennas Propagat.*, vol. AP-27, no. 6, pp. 808–813, 1979.

[2] M. I. Herman and J. L. Volakis, "High-frequency scattering by a resistive strip and extensions to conductive and impedance strips," *Radio Sci.*, vol. 22, no. 3, pp. 335–349, 1987.

[3] R. Tiberio, F. Bessi, G. Manara, and G. Pelosi, "Scattering by a strip with two face impedances at edge-on incidence," *Radio Sci.*, vol. 17, no. 5, pp. 1199–1210, 1982.

[4] E. I. Veliev, K. Kobayashi, T. Ikiz, and S. Koshikawa, "Analytical-numerical approach for the solution of the diffraction by a resistive strip," Paper presented at *1996 International Symposium on Antennas and Propagation*, September 24–27, 1996, Chiba, Japan.

[5] E. I. Veliev and V. V. Veremey, "Numerical-analytical approach for the solution to the wave scattering by polygonal cylinders and flat strip structures," in *Analytical and Numerical Methods in Electromagnetic Wave Theory*, Chap. 10, M. Hashimoto, M. Idemen, O. A. Tretyakov, Eds., Science House, Tokyo, 1993.

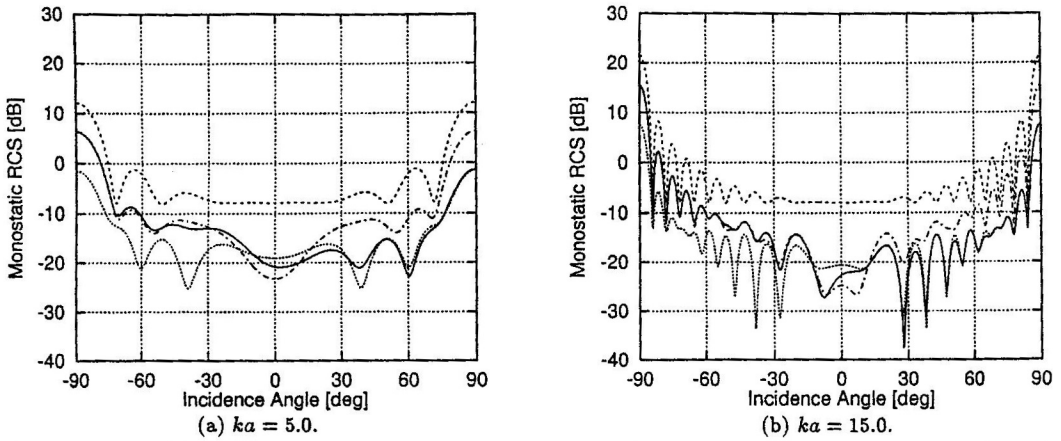

(a) $ka = 5.0$. (b) $ka = 15.0$.

Fig. 2. Monostatic RCS. – – – – –: $\zeta_1 = \zeta_2 = 0.0$; ————: $\zeta_1 = 1.5$, $\zeta_2 = 3.0$; ·····: $\zeta_1 = \zeta_2 = 1.5$; – · – · – · –: $\zeta_1 = \zeta_2 = 3.0$.

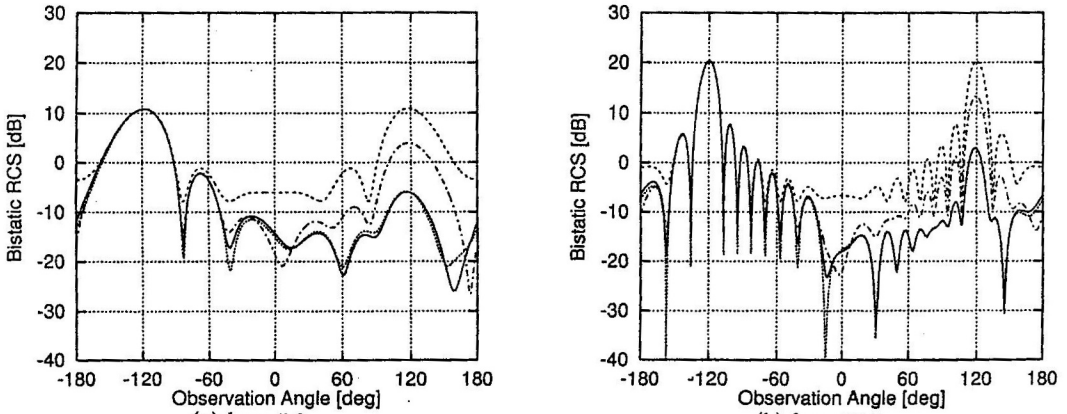

(a) $ka = 5.0$. (b) $ka = 15.0$.

Fig. 3. Bistatic RCS for $\theta = 60°$. – – – – – –: $\zeta_1 = \zeta_2 = 0.0$; ————: $\zeta_1 = 1.5$, $\zeta_2 = 3.0$; ·····: $\zeta_1 = \zeta_2 = 1.5$; – · – · – · –: $\zeta_1 = \zeta_2 = 3.0$.

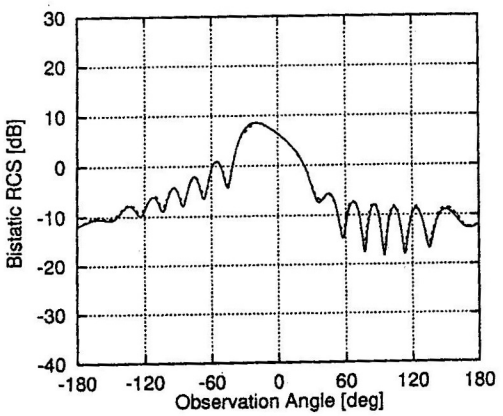

Fig. 4. Bistatic RCS for $\theta = 180°$, $ka = 10.0$, $\zeta_1 = 4.0$, $\zeta_2 = 0.0$ and its comparison with Tiberio *et al.* [3]. ————: this paper; – – – – – –: Tiberio *et al.*